

Paramagnetic squeezing of QCD matter

G. S. Bali,^{1,2} F. Bruckmann,¹ G. Endrődi,^{1,*} and A. Schäfer¹

¹*Institute for Theoretical Physics, Universität Regensburg, D-93040 Regensburg, Germany*

²*Department of Theoretical Physics, Tata Institute of Fundamental Research, Homi Bhabha Road, Mumbai 400005, India.*

We determine the magnetization of Quantum Chromodynamics (QCD) for several temperatures around and above the transition between the hadronic and the quark-gluon phases of strongly interacting matter. We obtain a paramagnetic response that increases in strength with the temperature. We argue that due to this paramagnetism, chunks of quark-gluon plasma produced in non-central heavy ion collisions should become elongated along the direction of the magnetic field. This anisotropy will then contribute to the elliptic flow v_2 observed in such collisions, in addition to the pressure gradient that is usually taken into account. We present a simple estimate for the magnitude of this new effect and a rough comparison to the effect due to the initial collision geometry. We conclude that the paramagnetic effect might have a significant impact on the value of v_2 .

1. INTRODUCTION

In heavy-ion collisions (HICs) strongly interacting matter is exposed to extreme conditions to probe the QCD phase diagram and to reveal properties of the quark-gluon plasma (QGP). It is however not straightforward to relate characteristics of the so produced QCD medium to experimental signatures. One of the most prominent experimental observables is the elliptic flow v_2 [1], which marks the onset of hydrodynamic behavior at very early times (hydroization). Connecting v_2 to the centrality of HICs in a model-independent way is crucial to extract the ratio of viscosity to entropy density η/s of the QGP [2].

Another important aspect of the initial phase of HICs is the generation of extremely strong magnetic fields [3–6]. We show that these magnetic fields may have an impact on v_2 and, therefore, should be taken into account in a quantitative analysis of the elliptic flow. Irrespective of this observable effect, the response to magnetic fields is a fundamental property of QCD matter which deserves to be studied in its own right. Other applications of our findings include models of neutron stars (magnetars [7]) and primordial magnetic fields in the early universe (see, e.g., Ref. [8]).

All information about the response of QCD to magnetic fields can be deduced from the free energy density $f = -T/V \cdot \log \mathcal{Z}$, given in terms of the partition function \mathcal{Z} . Applying a constant external magnetic field B induces a nonzero magnetization

$$M = -\frac{\partial f}{\partial(eB)}, \quad (1)$$

which we normalized by the elementary charge ($e > 0$). The sign of M determines whether the QCD vacuum as a medium exhibits a *paramagnetic* response ($M > 0$) or a *diamagnetic* one ($M < 0$) [9]. In the former case the magnetization is aligned parallel to the external field,

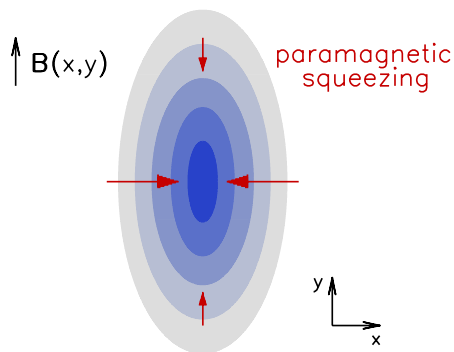


FIG. 1: Typical magnetic field profile in the transverse plane of a non-central heavy-ion collision (darker colors represent stronger fields). The paramagnetic squeezing exerts the force indicated by the red arrows. As a result, the QGP is elongated in the y -direction.

while in the latter case it is antiparallel. One clue about the sign of M came from a low-energy effective model of QCD — the hadron resonance gas (HRG) model — which predicted the magnetization to be positive and thus the QCD vacuum to be a paramagnet [10]. Several methods were since developed to study the problem on the lattice [11–14]. All of the results agree qualitatively, confirming the finding of the HRG model that the QCD vacuum is *paramagnetic*.

In the present letter we extend the lattice measurements of Ref. [11] to cover several temperatures in and above the transition region. We do not yet provide final, continuum extrapolated values for the magnetization, but instead aim at a first estimate of the effect of QCD paramagnetism on the phenomenology of heavy ion collisions. To this end, let us consider a chunk of the QGP exposed to a non-uniform magnetic field. Owing to the positivity of M , the free energy is minimized when the medium is located in regions where B is maximal. The minimization of f thus results in a net force, which strives to change the shape of the medium. For a non-central HIC (with \hat{z} being the direction of the collision axis, \hat{x} - \hat{z} the reaction plane and \hat{y} the direction of the magnetic field induced by the beams), this force will elongate the distribution of QCD matter along the y -direction, see

*Corresponding author, email: gergely.endrodi@physik.uni-r.de

Fig. 1. This elongation can affect the azimuthal structure of the expansion of the system, in addition to the pressure gradients due to the initial geometry. We call this effect *paramagnetic squeezing*.

The interplay of the geometric pressure gradient and the paramagnetic squeezing crucially depends both on the time- and space-dependence of the magnetic field [15, 16] and on the moment of the onset of early hydroization [17]. Both time scales are subjects of ongoing debate. We also remark that our quantitative results apply, strictly speaking, to QCD matter in thermal equilibrium only. Therefore, at present the best we can do is to estimate whether the impact of the sketched squeezing effect is sizeable. According to our numerical results, which we detail below, this can be the case for RHIC and in particular for LHC collisions. This clearly calls for a quantitative analysis of the dynamics of the decay of the initial magnetic field and of the on-set of hydroization.

We mention that the paramagnetic squeezing may correlate the recently observed large event-by-event fluctuations in v_2 [18] with fluctuations of the magnetic field. Furthermore, we note that a similar squeezing effect may operate in the inner core of magnetars if the magnetic field there reaches typical QCD scales ($B \sim 10^{14-15}$ T).

2. LATTICE SETUP

We consider a hypercubic lattice of size $N_s^3 \times N_t$ and spacing a . The discretization of the QCD action we choose is the tree-level Symanzik improved gluonic action and stout smeared staggered quarks for the three lightest flavors (the detailed simulation setup is described in Refs. [19, 20]). The quark masses are set to their physical values along the line of constant physics (for details see Ref. [21]), $m_u = m_d = m_s/28.15$. The electric charges of the quarks are $q_u/2 = -q_d = -q_s = e/3$. The flux Φ of the magnetic field on the lattice is quantized,

$$\Phi \equiv (N_s a)^2 \cdot eB = 6\pi N_b, \quad N_b \in \mathbb{Z}, \quad 0 \leq N_b < N_s^2, \quad (2)$$

which prohibits the direct evaluation of the magnetization, Eq. (1), as a derivative with respect to B . The first approach to circumvent this problem was developed in Ref. [11], where we calculated M as the difference of lattice pressures parallel and perpendicular to B . Several alternatives were also introduced recently to determine the magnetization. In Refs. [12], the derivative of f with respect to B is constructed (giving an unphysical quantity due to flux quantization) and then integrated to obtain the physical change of the free energy due to B . Ref. [13] evades flux quantization altogether by considering a magnetic field which is positive in one and negative in the other half of the lattice. Finally, in Ref. [14] we developed an integral method which is based on the B -independence of f at asymptotically large quark masses.

Here we follow the approach of Ref. [11]. The main idea is the following: Flux quantization implies that a

hypothetical compression of the system in the direction perpendicular to B can only proceed keeping Φ fixed – which automatically implies changing B . Therefore, one has to compress the magnetic field lines together with the system. In Ref. [11] we have shown that this gives a consistency relation between the response of the system to a change in B – i.e., the magnetization – and the response to a change in the size of the system in different directions – i.e. the pressures. This leads to the relation

$$-M \cdot eB = -(\zeta_g + \hat{\zeta}_g) \cdot [A(\mathcal{B}) - A(\mathcal{E})] - \zeta_f \cdot \sum_f A(\mathcal{C}_f), \quad (3)$$

where $A(\mathcal{B})$, $A(\mathcal{E})$ are the anisotropies in the chromomagnetic and chromoelectric parts of the gluonic action, $A(\mathcal{C}_f)$ is the anisotropy in the fermionic action for the quark flavor f ($f = u, d, s$), and ζ_g , $\hat{\zeta}_g$ and ζ_f are renormalization coefficients that may be determined, e.g., by simulating on anisotropic lattices. To leading order in perturbation theory, $\zeta_g = \hat{\zeta}_g = \zeta_f = 1$. We found the gluonic anisotropies to be by factors of 5–10 smaller than the fermionic anisotropy. This means that the magnetization is well approximated by $M \cdot eB \approx \sum_f A(\mathcal{C}_f)$, within a systematic error of 10–20 %. The fermionic anisotropy in terms of the parallel and perpendicular components of the Dirac operator reads

$$A(\mathcal{C}_f) = \frac{1}{2} [\bar{\Psi}_f \not{D}_x \Psi_f + \bar{\Psi}_f \not{D}_y \Psi_f] - \bar{\Psi}_f \not{D}_z \Psi_f, \quad (4)$$

where \not{D}_μ is the component of the Dirac operator proportional to γ_μ , which is readily accessible on the lattice.

3. RENORMALIZATION

The free energy in the presence of an external magnetic field contains a B -dependent logarithmic divergence. This divergence stems from the coupling of quarks to B through their electric charges and is cancelled by the renormalization of the electric charge [22]. The fact that

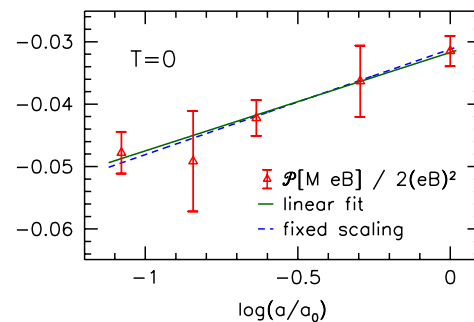


FIG. 2: The divergent $\mathcal{O}((eB)^2)$ contribution to the magnetization normalized by $2(eB)^2$, as a function of the logarithm of the lattice spacing (in units of $a_0 = 1.47 \text{ GeV}^{-1}$, our coarsest lattice). A linear fit with two free parameters (green solid line) and one with the slope fixed to the leading perturbative prediction β_1^{QED} (see text) is also shown (dashed blue line).

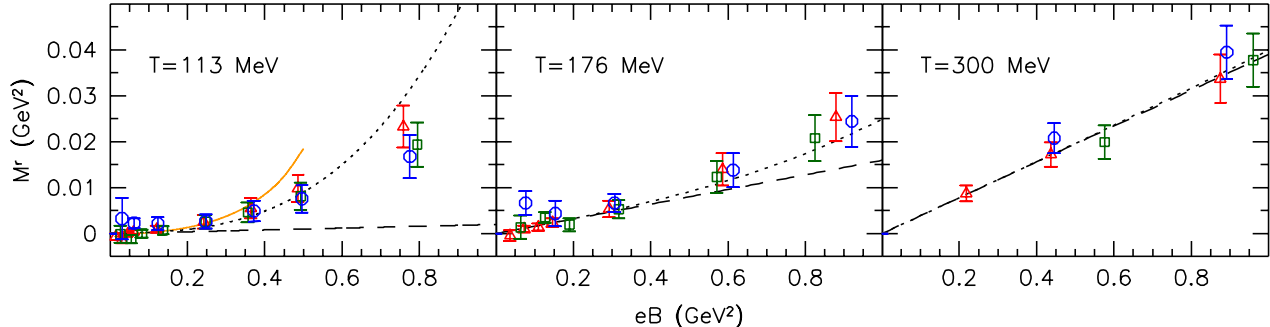


FIG. 3: Renormalized magnetization of QCD as a function of the magnetic field for various values of temperature. Different colors encode different lattice spacings: $N_t = 6$ (red triangles), $N_t = 8$ (green squares) and $N_t = 10$ (green circles). The continuum limit corresponds to $N_t \rightarrow \infty$. Below T_c we show the HRG model prediction [10] (solid orange line). The dashed lines represent the linear terms in M^r , which were determined by fitting the magnetization at small magnetic fields, whereas the dotted curves show the results of cubic fits.

the prefactor of the divergence in question is given by the lowest-order QED β -function coefficient β_1 (this contains perturbative and non-perturbative QCD corrections) further illustrates the fundamental relation between the B -dependent divergence of f and electric charge renormalization. At zero temperature, this divergence constitutes the only term which is of $\mathcal{O}((eB)^2)$:

$$f(B) - f(0) = -\beta_1 \cdot (eB)^2 \cdot \log(a) + \mathcal{O}((eB)^4). \quad (5)$$

The magnetization inherits this divergence and – again, at zero temperature – has the structure

$$M \cdot eB = 2\beta_1 \cdot (eB)^2 \cdot \log(a) + \mathcal{O}((eB)^4). \quad (6)$$

The renormalization of M therefore amounts to subtracting the total $\mathcal{O}((eB)^2)$ term at zero temperature (for a more detailed explanation of this point see, e.g., Refs. [10, 23]). This term can be determined by considering the limit of small magnetic fields. This results in the renormalization prescription

$$f^r = (1 - \mathcal{P})[f], \quad M^r \cdot eB = (1 - \mathcal{P})[M \cdot eB], \quad (7)$$

where \mathcal{P} is the operator that projects out the $\mathcal{O}((eB)^2)$ term from an observable X :

$$\mathcal{P}[X] = (eB)^2 \cdot \lim_{eB \rightarrow 0} \frac{X}{(eB)^2}. \quad (8)$$

In Fig. 2 we show the coefficient of the divergent term $\mathcal{P}[M \cdot eB]/2(eB)^2$ for several lattice spacings at $T = 0$. In accordance with Eq. (6), the divergent term is found to be proportional to $\log(a)$, with a coefficient of 0.016(4). The leading order perturbative scaling is given by the lowest order coefficient of the QED β -function for three quark flavors with $N_c = 3$ colors, $\beta_1^{\text{QED}} = N_c/(12\pi^2) \cdot \sum_{f=u,d,s} (q_f/e)^2 \approx 0.0169$: the fitted slope is consistent with the perturbative prediction, within statistical errors. Increasing the statistics would be necessary to resolve QCD corrections to β_1 .

4. RESULTS AND DISCUSSION

We can now subtract the divergent part of M measured at $T = 0$ to obtain the temperature-dependence of the renormalized magnetization M^r , as defined in Eq. (7). The result is shown in Fig. 3, where M^r is plotted for $eB < 1.0 \text{ GeV}^2$ at three values of the temperature. The results for all three lattice spacings fall essentially on top of each other, indicating small lattice artefacts. (Note that the renormalization at $T = 300 \text{ MeV}$, where the lattice spacing is the smallest, requires an extrapolation of the $T = 0$ contribution of Fig. 2. The systematic error due to this extrapolation is taken into account here.)

We find $M^r > 0$ for all temperatures, which demonstrates the paramagnetic nature of the thermal QCD vacuum. This is in agreement with our earlier results at $T = 0$ [11]. Note that the expansion of M^r in the magnetic field at $T = 0$ starts as $(eB)^3$. As the temperature increases, thermal contributions induce an additional linear term in M^r , as is visible in the plots (shown by the dashed lines). This behavior is also present in the HRG model prediction, which we include in the figure for the lowest temperature, where the hadronic description is expected to be still valid. We find the HRG model to reproduce the lattice data for small fields $eB \lesssim 0.3 \text{ GeV}^2$.

The results are well described by a cubic function $M^r = \chi_1 \cdot eB + \chi_3 \cdot (eB)^3/T^4$, shown by the dotted lines in Fig. 3. The linear coefficient is the magnetic susceptibility, marking the leading response of QCD to the external field. It is zero at low temperatures and increases drastically above the transition. On the other hand, the cubic term is found to decay strongly with temperature, consistent with T^{-4} as expected on dimensional grounds. The fit parameters are listed in Table I. We remark that for high temperatures we expect χ_1 to show a logarithmic rise with T ; the Stefan-Boltzmann limit of χ_1 for free massive quarks is $2\beta_1^{\text{QED}} \cdot \log(T/m)$ [24]. (Note that such an entanglement between ultraviolet and infrared divergences for nonzero magnetic fields is well-known, see, e.g., Ref. [25].) The high-temperature limit of the next

T (MeV)	113	130	142	176	300
$\chi_1 \cdot 10^2$	0.2(5)	0.4(7)	1.1(6)	1.6(5)	3.9(6)
$\chi_3 \cdot 10^6$	9(5)	8(3)	6(3)	9(5)	7(5)

TABLE I: Temperature-dependence of the coefficients χ_1 and χ_3 . To obtain the (linear) magnetic susceptibility in SI units, one needs to multiply χ_1 by $e^2 \approx 4\pi/137$.

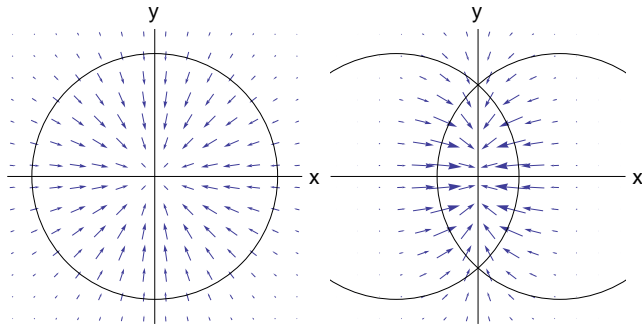


FIG. 4: Paramagnetic force profiles for typical central (left panel) and peripheral (right panel) heavy-ion collisions. The circles represent the colliding nuclei.

coefficient is $\chi_3 = 31N_c \zeta(5)/(960\pi^6) \cdot \sum_{f=u,d,s} (q_f/e)^4 \approx 2.32 \cdot 10^{-5}$, with a negative m^2/T^2 correction [26]. The lattice data indeed approaches this limit from below.

We are now in the position to discuss the implications of our results on HIC phenomenology. For a non-uniform magnetic field, the paramagnetic squeezing is manifested by a force density F^{ps} , which arises as the system strives to minimize its free energy,

$$F^{\text{ps}} = -\nabla f^r = -\frac{\partial f^r}{\partial (eB)} \cdot \nabla (eB) = M^r \cdot \nabla |eB|. \quad (9)$$

Note that the free energy density – being a Lorentz-scalar – is only sensitive to the magnitude of the field, which allowed us to replace eB by $|eB|$ above. Motivated by model descriptions of the magnetic field profile [5, 6], we consider a simple two-dimensional Gaussian distribution of the magnetic field (with widths $\sigma_x = \sigma_y$ for a central collision and $\sigma_x = \sigma_y/2$ for a peripheral collision). The so obtained force profiles are depicted in Fig. 4. While isotropic for central collisions, this inward-pointing force becomes anisotropic for the peripheral case, squeezing and hence elongating the medium distribution.

At high temperatures the magnetization is linear in eB (see the right panel of Fig. 3), and the gradient also contains a factor of eB , making F^{ps} proportional to the square of the magnetic field. Accordingly, the effect is very sensitive to the spatial profile of the magnetic field generated in the collision. Furthermore, this profile de-

pends strongly on the time elapsed since the moment of the collision [15], giving rise to a complex behavior of the squeezing effect as a function of space and time.

We now make a first attempt to estimate the strength of the paramagnetic squeezing effect based on very simplistic assumptions, and quantify it in terms of the difference between the magnitudes of the force densities acting at $(\sigma_x, 0)$ and at $(0, \sigma_y)$. This is equivalent to a difference Δp^{ps} of pressure gradients. From our results for the magnetization at $T = 300$ MeV and the magnetic field profiles of Refs. [5, 6], we obtain $|\Delta p^{\text{ps}}| \approx 0.007$ GeV/fm⁴ for magnetic fields of the order of $5m_\pi^2$ (the typical value obtained in model calculations for RHIC energies [5, 6, 27]). Using the magnetic field $50m_\pi^2$ corresponding to LHC energies [6] amounts to $|\Delta p^{\text{ps}}| \approx 0.7$ GeV/fm⁴. Similar estimates for the early-time pressure gradients p^g resulting from the geometric effect give differences of $|\Delta p^g| \approx 0.1$ GeV/fm⁴ for RHIC and $|\Delta p^g| \approx 1$ GeV/fm⁴ for LHC energies [28], see also Refs. [29]. The estimates for the paramagnetic squeezing are subject to large systematic errors originating, for example, from the uncertainty of the QGP electric conductivity [15, 16]. Moreover, due to the complex space- and time-dependence of both mechanisms, a comparison based only on the magnitude of F^{ps} at two spatial points is clearly too simplistic. Instead, one should consider a model for the early stage ($t \lesssim 1$ fm/c) of the collision, and take the paramagnetic squeezing effect into account from the beginning. This is outside the scope of the present letter.

To summarize: we have studied the magnetic response of the quark-gluon plasma by means of lattice simulations at physical quark masses. The response is *paramagnetic* and the magnetization at different temperatures is plotted in Fig. 3 and parameterized in Table I. Based on these equilibrium results we estimated the *paramagnetic squeezing* effect on chunks of quark-gluon plasma produced in heavy ion collisions. We compared its magnitude to pressure gradients arising from geometrical effects. The energy-dependence of the two mechanisms is quite different. For typical HICs at RHIC we found the paramagnetic squeezing to give a 10% correction to the geometric effect, while for LHC collisions they are similar in size. Our estimates should be improved by more involved model calculations of the elliptic flow, taking into account the paramagnetic squeezing in the evolution of the fireball. As both the onset of hydroization and the magnetic field dynamics are still subject of debates, this calls for a dedicated large scale effort.

Acknowledgements. Our work was supported by the DFG (SFB/TRR 55), the EU (ITN STRONGnet 238353) and the Alexander von Humboldt Foundation. The authors thank Pasi Huovinen, Simon Mages, Berndt Müller and Hannah Petersen for useful discussions.

[1] L. Csernai and D. Rohrlich *Phys.Lett.* **B458** (1999) 454, [[nucl-th/9908034](#)].

[2] P. Romatschke and U. Romatschke *Phys.Rev.Lett.* **99**

- (2007) 172301, [[arXiv:0706.1522](#)].
- [3] V. Skokov, A. Y. Illarionov, and V. Toneev *Int. J. Mod. Phys. A* **24** (2009) 5925–5932, [[arXiv:0907.1396](#)].
- [4] A. Bzdak and V. Skokov *Phys.Lett. B* **710** (2012) 171–174, [[arXiv:1111.1949](#)].
- [5] V. Voronyuk, V. Toneev, W. Cassing, E. Bratkovskaya, V. Konchakovski, et al. *Phys.Rev. C* **83** (2011) 054911, [[arXiv:1103.4239](#)].
- [6] W.-T. Deng and X.-G. Huang *Phys.Rev. C* **85** (2012) 044907, [[arXiv:1201.5108](#)].
- [7] R. C. Duncan and C. Thompson *Astrophys. J.* **392** (1992) L9.
- [8] D. Grasso and H. R. Rubinstein *Phys.Rept.* **348** (2001) 163–266, [[astro-ph/0009061](#)].
- [9] L. Landau, E. Lifshitz, and L. Pitaevskii, vol. VIII. of *Course of theoretical physics*. Butterworth-Heinemann, 1995. Paragraph 31.
- [10] G. Endrődi *JHEP* **1304** (2013) 023, [[arXiv:1301.1307](#)].
- [11] G. Bali, F. Bruckmann, G. Endrődi, F. Gruber, and A. Schäfer *JHEP* **1304** (2013) 130, [[arXiv:1303.1328](#)].
- [12] C. Bonati, M. D’Elia, M. Mariti, F. Negro, and F. Sanfilippo [arXiv:1307.8063](#); C. Bonati, M. D’Elia, M. Mariti, F. Negro, and F. Sanfilippo [arXiv:1310.8656](#).
- [13] L. Levkova and C. DeTar [arXiv:1309.1142](#).
- [14] G. Bali, F. Bruckmann, G. Endrődi, and A. Schäfer [arXiv:1310.8145](#).
- [15] K. Tuchin *Phys.Rev. C* **88** (2013) 024911, [[arXiv:1305.5806](#)].
- [16] L. McLerran and V. Skokov [arXiv:1305.0774](#).
- [17] M. P. Heller, R. A. Janik, and P. Witaszczyk *Phys.Rev.Lett.* **108** (2012) 201602, [[arXiv:1103.3452](#)]; W. van der Schee, P. Romatschke, and S. Pratt [arXiv:1307.2539](#).
- [18] ALICE Collaboration, A. R. Timmins *J.Phys.Conf.Ser.* **446** (2013) 012031, [[arXiv:1301.6084](#)].
- [19] Y. Aoki, Z. Fodor, S. Katz, and K. Szabó *JHEP* **0601** (2006) 089, [[hep-lat/0510084](#)].
- [20] G. Bali, F. Bruckmann, G. Endrődi, Z. Fodor, S. Katz, et al. *JHEP* **1202** (2012) 044, [[arXiv:1111.4956](#)].
- [21] S. Borsányi, G. Endrődi, Z. Fodor, A. Jakovác, S. D. Katz, et al. *JHEP* **1011** (2010) 077, [[arXiv:1007.2580](#)].
- [22] J. S. Schwinger *Phys.Rev.* **82** (1951) 664–679.
- [23] P. Elmfors, D. Persson, and B.-S. Skagerstam *Astropart.Phys.* **2** (1994) 299–326, [[hep-ph/9312226](#)]; G. V. Dunne [hep-th/0406216](#).
- [24] P. Elmfors, D. Persson, and B.-S. Skagerstam *Phys.Rev.Lett.* **71** (1993) 480–483, [[hep-th/9305004](#)].
- [25] G. V. Dunne, H. Gies, and C. Schubert *JHEP* **0211** (2002) 032, [[hep-th/0210240](#)].
- [26] D. Cangemi and G. V. Dunne *Annals Phys.* **249** (1996) 582–602, [[hep-th/9601048](#)].
- [27] J. Błoczyński, X.-G. Huang, X. Zhang, and J. Liao *Phys.Lett. B* **718** (2013) 1529–1535, [[arXiv:1209.6594](#)].
- [28] P. Huovinen. private communication.
- [29] P. F. Kolb, J. Sollfrank, and U. W. Heinz *Phys.Rev. C* **62** (2000) 054909, [[hep-ph/0006129](#)]; H. Petersen, Q. Li, X. Zhu, and M. Bleicher *Phys.Rev. C* **74** (2006) 064908, [[hep-ph/0608189](#)].